

1 **A potential suite of climate markers of long-chain *n*-alkanes and alkenones**
2 **preserved in the top sediments from the Pacific sector of the Southern Ocean**

3

4 Xin Chen^{1,3*}, Xiaodong Liu¹, Da-Cheng Lin², Jianjun Wang³, Liqi Chen³, Pai-Sen Yu⁴,
5 Linmiao Wang⁵, Zhifang Xiong⁵, Min-Te Chen^{2,6*}

6

7 ¹ Anhui Province Key Laboratory of Polar Environment and Global Change, School
8 of Earth and Space Sciences, University of Science and Technology of China, Hefei,
9 Anhui 230026, China

10 ² Institute of Earth Sciences & Center of Excellence for the Oceans & Center of
11 Excellence for Ocean Engineering, National Taiwan Ocean University, Keelung,
12 20224, Taiwan

13 ³ Key Laboratory of Global Change and Marine - Atmospheric Chemistry (GCMAC)
14 of Ministry of Natural Resources (MNR), Third Institute of Oceanography (TIO),
15 MNR, Xiamen 361005, China

16 ⁴ Taiwan Ocean Research Institute, National Applied Research Laboratories,
17 Kaohsiung 80143, Taiwan

18 ⁵ Key Laboratory of Marine Geology and Metallogeny, First Institute of
19 Oceanography, Ministry of Natural Resources, Qingdao 266061, China

20 ⁶ Pilot National Laboratory for Marine Science and Technology, Qingdao 266061,
21 China

22

23 *Corresponding author: Xin Chen (chenxust@mail.ustc.edu.cn) and Min-Te Chen
24 (mtchen@ntou.edu.tw)

25

26 **Abstract**

27

28 Investigation of organic compounds in marine sediments can potentially unlock a
29 wealth of new information in these overlooked climate archives. Here we present pilot
30 study results of organic geochemical features of long-chain *n*-alkanes and alkenones
31 and individual carbon isotope ratios of long-chain *n*-alkanes from a newly collected,
32 approximately 8-meter long, Pleistocene age sediment core, located in the far reaches
33 of the Pacific sector of the Southern Ocean. We initially analyzed a suite of organic
34 compounds in the core, and the results show abundant long-chain *n*-alkanes (C₂₉-C₃₅)
35 with predominant odd-over-even carbon preference, which suggests an origin of
36 terrestrial higher plant waxes via long range transport of dust, possibly from Australia
37 and New Zealand. The $\delta^{13}\text{C}$ values of the C₃₁ *n*-alkane range from -29.4 to -24.8‰, in
38 which the higher $\delta^{13}\text{C}$ values suggest more contributions from C₄ plants waxes. In the
39 analysis, we found that the mid-chain *n*-alkanes (C₂₃-C₂₅) have small odd-over-even
40 carbon preference, suggesting that they were derived from marine non-diatom pelagic
41 phytoplankton and microalgae, and terrestrial sources. Furthermore, the C₂₆ and C₂₈
42 with lower $\delta^{13}\text{C}$ values (~ -34‰) indicate an origin from marine chemoautotrophic
43 bacteria. We found that the abundances of tetra-unsaturated alkenones (C_{37:4}) in this
44 Southern Ocean sediment core ranges from 11-37%, perhaps a marker of low sea
45 surface temperature (SST). The results of this study strongly indicate that the $\delta^{13}\text{C}$
46 values of long-chain *n*-alkanes and U₃₇^k index are potentially useful to reconstruct
47 detailed history of C₃/C₄ plants and SST change in the higher latitudes of the Southern
48 Ocean.

49

50 Keywords: Southern Ocean; Pacific Ocean; *n*-alkane; carbon isotopic; SST; U_{37}^k

51 1. Introduction

52
53 The Southern Ocean plays an important role in global climate and carbon cycle related to westerly
54 winds and the Antarctic Circumpolar Current (ACC, Fischer et al. 2010; Marshall and Speer 2012).
55 Mid-latitude westerly winds are important in transporting mineral dust from the continent of Australia and
56 New Zealand to the South Pacific sector of the Southern Ocean (Lamy et al. 2014). The location and
57 intensive change of the westerly winds and ACC directly control the exchange of heat, salt, nutrients and
58 freshwater between low and high latitudes (Pahnke and Zahn 2005; Toggweiler and Russell 2008;
59 Shevenell et al. 2011; Toyos et al. 2020). Thus, environmental fluctuations in the Southern Ocean play a
60 vital role in global climate change.

61 Well preserved organic matter in marine sediments is a direct indicator of environmental conditions at
62 the time of sedimentation and thus is important for paleo-environmental studies (Meyers and Ishiwatari
63 1993). Among these, lipid organic biomarkers have been widely used to reconstruct past environmental
64 and climatic conditions in oceans and lakes (Eglinton and Eglinton 2008; Holtvoeth et al. 2019).
65 Long-chain *n*-alkanes (C₂₅-C₃₅) are important components of the epicuticular wax in higher terrestrial
66 plants, and these *n*-alkanes are eroded from leaf surfaces and soil by winds and then transported to the
67 Southern Ocean (Bendle et al. 2007; Martínez-García et al. 2009, 2011; Lamy et al. 2014; Jaeschke et al.
68 2017). Short- and mid-chain lengths have been reported as the major components of *n*-alkanes in the
69 surface ocean sediments around Antarctica, carbon preference index (CPI) and specific-compound carbon
70 isotopic values have also been reported to be mainly derived from phytoplankton and bacteria (Harada et
71 al. 1995; Bubba et al. 2004). Relatively higher carbon isotopic values of C₃₁ *n*-alkane in the surface
72 sediments from the Australian sector of the Southern Ocean suggest significant contributions of C₄ higher
73 vascular plant waxes or conifer resin (Ohkouchi et al. 2000). Altered or recycled material mixed with
74 modern marine input is also an important source for long-chain *n*-alkanes with low CPI values in ocean
75 sediments in the Ross Sea region (Kvenvolden et al. 1987; Venkatesan 1988; Duncan et al. 2019).
76 Although the high latitude of the Southern Ocean is usually considered to be little influenced by river and
77 continent soils, based on above results, the sources of *n*-alkanes in the ocean sediments are thought to be
78 complex, thus their eco-environmental implications are still being explored.

79 A subtropical to polar SST gradient has been related to the position and intensity of the westerly
80 winds and ACC in the Southern Ocean (Lamy et al. 2010; Kohfeld et al. 2013). Therefore, quantitative
81 SST records from the past are essential for evaluating the importance of the Southern Ocean for the global
82 climate. However, the most widely used organic geochemical SST index, alkenone paleothermometry, has

only rarely been employed in high latitudes of the Southern Ocean. The $U_{37}^k = ([C_{37:2} - C_{37:4}] / [C_{37:2} + C_{37:3} + C_{37:4}])$ index has been proposed to quantify the degree of alkenone unsaturation (Brassell et al. 1986), which is a function of SST. Because trace of $C_{37:4}$ is often absent in open ocean sediments when SSTs are higher than 12°C (Prah and Wakeham 1987), the index was simplified to $U_{37}^{k'} = ([C_{37:2}] / [C_{37:2} + C_{37:3}])$. In recent decades, the $U_{37}^{k'}$ index has been widely used at middle and low latitudes marine environments. However, our knowledge on the application of alkenone paleothermometry in the high latitudes of the Southern Ocean is still largely insufficient. Only a few examples exist, such as that $C_{37:4}$ methyl alkenone was not detected in the 10-12°C waters, and even in the 1.5°C waters the abundance was still very minor (Sikes and Volkman 1993), while it was detected in most surface sediment samples at 3.5°C in spring cruise samples in the Southern Ocean (Sikes et al. 1997). The $U_{37}^{k'}$ index is more proper than U_{37}^k when used in sea surface temperature estimations, even in cold conditions (Sikes et al. 1997; Jaeschke et al. 2017). However, Ho et al. (2012) found that there was a significant warming trend between the glacial and inter-glacial periods inferred from $U_{37}^{k'}$ records in the subantarctic, with the discrepancy due to the relative high abundance of the $C_{37:4}$ alkenones during cold intervals. Data on alkenone paleothermometry is still largely lacking and these various results of U_{37}^k and $U_{37}^{k'}$ -SSTs indicate that more investigations are still needed in the high latitudes of the Southern Ocean.

Considering the importance of the position and strength of westerly winds and the Antarctic Circumpolar Current, reconstructing surface ocean hydroclimatic changes using organic biomarkers (e.g., long-chain *n*-alkanes and alkenones) has been very necessary for better understanding the role of the Southern Ocean in the context of global climate change. Before carrying out such work, it is firstly important to determine the source of organic matter and to estimate whether the U_{37}^k index could be useful or not in the Southern Ocean. Here, we analyze the organic geochemical features of long-chain *n*-alkanes, alkenones and the compound-specific carbon isotope (long-chain *n*-alkanes C_{23} - C_{31}) in the ocean sediments from one core in the South Pacific sector of the Southern Ocean (66°13'47.16"S, 168°11'8.34"E). Our main objectives are: (a) to evaluate the source of long-chain *n*-alkanes based on their chain length distributions and individual carbon isotopes, (b) to report the distributional features of di-, tri- and tetra-unsaturated alkenones, and (c) to assess the applicability of the alkenones indices in the high latitudes of the Southern Ocean for the reconstruction of paleoclimate change and the possible prediction of climate in the future.

2. Materials and methods

2.1 Materials

The gravity core R23 was drilled at 168°11'8.34"E, 66°13'47.16"S at a water depth of 2967 m during the "31th Chinese National Antarctic Research Expedition (CHINARE)" cruise in 2014-2015 (Fig. 1). The sediment core is 819 cm long, with a top 10 cm soupy layer that is characterized by high water content. The core was subsampled at an interval of 2 cm. The color of the sediments varies among olive, brown and gray throughout the profile. Based on the wet and dry sieving experiments, the core mainly consists of homogenous clay with minor proportions of sand (63-2000 μm), some ice-rafted debris (IRD; >2 mm) and some foraminifera are randomly found, but sponge spicules present throughout the core with relatively high abundance. No obvious bioturbations were observed in this core. The lack of planktonic foraminiferal CaCO_3 in these regional marine sediments makes it difficult to rapidly establish an age model using traditional oxygen isotope method. However, the precise chronological framework of the R23 core can be obtained with the comparison of high-resolution Ba/Ti ratios with LR04 $\delta^{18}\text{O}$ curves (Lisiecki and Raymo 2005). The age of R23 core ranges from 3.4 to 330 ka from Wang et al. (unpublished data). In this pilot study, we only focus on the source identification of *n*-alkanes with different chain lengths, and then evaluate the possibility of C_{37} alkenones used as a suitable proxy for calculating the past sea surface temperature in this region. To study the potential of sedimentary organic geochemical features for paleoclimate reconstruction, we choose 12 samples at every ~ 80 cm interval for *n*-alkanes and alkenones analysis in this pilot study. All samples were stored under -20°C in the lab before analysis.

2.2 Lipids biomarker extraction

The lipids analysis procedure followed the methods of Yamamoto et al. (2000). Briefly, all sediment samples were freeze-dried, and then homogenized and powdered. Samples (2-3g) were weighed, and extracted two times with an Accelerated Solvent Extractor (DIONEX ASE 350) using dichloromethane-methanol (6:4 v/v) and then concentrated. The total lipid extract was separated into four fractions using column chromatography (SiO_2 with 5% distilled water; internal diameter, 5.5 mm; length, 45 mm) based on the degree of polarity: F1 (hydrocarbons, 4 ml hexane); F2 (aromatic hydrocarbons, 4 ml hexane-toluene (3:1 v/v)); F3 (ketones, 4 ml toluene); F4 (polar compounds, 4 ml toluene-methanol (3:1 v/v)). $\text{n-C}_{24}\text{D}_{50}$ and $\text{n-C}_{36}\text{H}_{74}$ were added as internal standards for the F1 and F3 fraction, respectively. Compounds were quantified using an internal standard ($\text{n-C}_{24}\text{D}_{50}$ and $\text{n-C}_{36}\text{H}_{74}$ for *n*-alkanes and alkenones, respectively) and by the proportional relation of the peak areas for each biomarker.

2.3 *n*-alkanes and alkenones analysis

Quantification of compounds was performed on a Hewlett Packard 6890 GC-FID system with a Chrompack DB-1MS column (length, 60 m; i.d., 0.25 mm; thickness, 0.25 μ m). The oven temperature was programmed from 70 to 290°C at 20°C/min, 290 to 310°C at 0.5°C/min, and then held at 310°C for more than 30 min. Helium was used as the carrier gas, with a flow rate of 30 cm/s. Selected samples were performed using GC-MS for compound identification, the GC column and oven temperature program was the same as GC-FID. The mass spectrometer was run in full scan mode (m/z 50–650). Electron ionization (EI) spectra were obtained at 70 eV. Alkenones were identified using an external standard by GC retention times by analogy with a synthetic standard (provided by M. Yamamoto, Hokkaido University, Japan) and characteristic mass fragments. *N*-alkanes were identified by comparing mass spectra and retention times with those of the standards and published data.

The carbon preference index (CPI; Bray and Evans 1961) of C_{26} - C_{34} homologues and the average chain length (ACL) of odd C_{27} - C_{35} homologues (Duan and He 2011) used in this study were as follows:

$$CPI = \left(\frac{C_{27} + C_{29} + C_{31} + C_{33}}{C_{26} + C_{28} + C_{30} + C_{32}} + \frac{C_{27} + C_{29} + C_{31} + C_{33}}{C_{28} + C_{30} + C_{32} + C_{34}} \right) / 2 \quad (1)$$

$$ACL = \frac{27 \times C_{27} + 29 \times C_{29} + 31 \times C_{31} + 33 \times C_{33} + 35 \times C_{35}}{C_{27} + C_{29} + C_{31} + C_{33} + C_{35}} \quad (2)$$

The $[C_{26}$ - $C_{35}]$ are concentration of odd and even *n*-alkane. The $U_{37}^k = ([C_{37:2}$ - $C_{37:4}] / [C_{37:2} + C_{37:3} + C_{37:4}])$ index has been proposed to quantify the degree of alkenone unsaturation (Brassell et al. 1986), which is a function of SST. Because $C_{37:4}$ is often absent in open ocean sediments when SSTs are higher than 12°C (Prah and Wakeham 1987), the index was simplified to $U_{37}^{k'} = ([C_{37:2}] / [C_{37:2} + C_{37:3}])$. We converted the index values to SST using the widely used *E. huxleyi* culture-based calibration proposed by Prah et al. (1988), $U_{37}^k = 0.04 T - 0.104$ ($r^2 = 0.98$) and $U_{37}^{k'} = 0.034 T + 0.039$ ($r^2 = 0.99$), and the simplified $U_{37}^{k'}$ calibration based on global core top compilations (Conte et al. 2006).

2.5 Carbon isotope analysis

The carbon isotope ratio of *n*-alkane was performed using a gas chromatograph with an DB-5MS column (60 m \times 320 μ m \times 250 μ m) interfaced to a Thermofisher MAT-253 isotope-ratio mass

179 spectrometer via a combustion interface (960°C) consisting of an alumina reactor containing nickel and
180 platinum wires. Helium was used as the carrier gas with a flow rate of 1.2ml/min using splitless injecting.
181 The oven temperature was programmed from 80 to 100 °C at 10°C/min, 100 to 220°C at 4°C /min, 220 to
182 280°C at 2°C/min, and then held at 280°C for 15mins. All samples are injected one time for carbon isotope
183 analysis. The analytical error was calculated based on the reproduced analytical results of an external
184 standard, injected once after every sixth sample injection, and had an analytical error of 0.7‰ (1σ). The
185 pre-calibrated isotopic composition of CO₂ was used as a standard. All δ¹³C values were expressed versus
186 VPDB.

187 Based on the isotopic values of *n*-alkanes, we can quantify the percentage source of long chain
188 *n*-alkanes from C₃/C₄ plants using a binary isotope mass balance model (Thomas et al. 2014):

$$\delta^{13}C_s = f \times \delta^{13}C_{C_3} + (1-f) \times \delta^{13}C_{C_4} \quad (3)$$

191
192 where δ¹³C_s are the long-chain *n*-alkanes from sediments, δ¹³C_{C₃} and δ¹³C_{C₄} are the carbon isotopic values
193 of long-chain *n*-alkanes from C₃ and C₄ terrestrial higher vascular plants, respectively, and f is the
194 proportion of long-chain *n*-alkanes from C₃ plants. We set the carbon isotopic values of long-chain
195 *n*-alkanes for C₃ and C₄ plants to be -36‰ and -22‰, respectively (Chikaraishi and Naraoka 2007). C₃₁
196 *n*-alkane abundance is relatively higher than C₂₉ and C₃₃ *n*-alkanes, thus, we use the carbon isotopic values
197 of C₃₁ *n*-alkane to calculate the percentage source of long-chain *n*-alkanes from C₃/C₄ plants.

199 3. Results

200 3.1 Concentration and distribution of long-chain *n*-alkanes

201
202
203 In the 12 pilot samples from the core R23, we found that there was a significant change in the
204 concentrations of total long-chain *n*-alkanes (C₂₃-C₃₅) in the sediment profile, ranging from 295-787 ng/g
205 (Table 1, Table S1). The distribution pattern of long-chain *n*-alkanes (C₂₃-C₃₅) in each sediment sample
206 was similar, with bimodal distributions peaking at C₂₃-C₂₅ and C₂₇ or C₃₁ (Fig. 2). However, there was no
207 obvious predominant odd-over-even carbon preference, and CPI₂₇₋₃₃ varied from 1.1-2.5, with an average
208 of 1.7. The distribution patterns of long-chain *n*-alkanes were divided into two types. One is mid-chain
209 *n*-alkanes (C₂₃-C₂₇), with no predominant odd-over-even carbon preference (CPI ~1), and the other is
210 long-chain *n*-alkanes (C₂₉-C₃₅) with predominant odd-over-even carbon preference. The ACL values of

211 long-chain *n*-alkanes (C₂₇-C₃₅) were in the range of 29.3-30.7. The ACL values are strongly correlated with
212 CPI (Fig. 3).

214 3.2 Concentration and distribution of alkenones

216 C_{37:4}, C_{37:3} and C_{37:2} alkenones were all detected in the 12 pilot samples, with total concentrations
217 ranging from 12.6-104.2 ng/g sediment dry wt (Table 2). The distribution pattern of three unsaturated
218 alkenones revealed significant differences among the subsamples, and the relative abundance of C_{37:4}, C_{37:3}
219 and C_{37:2} varied from 11-37%, 27-87% and 3-48%, respectively. The tri-unsaturated alkenone (C_{37:3}) was
220 the most abundant alkenone in the sediments. Interestingly, a high abundance of tetra-unsaturated alkenone
221 was found in the sediment samples. The SST estimates inferred from the U₃₇^k and U₃₇^{k'} indexes are
222 between -1.7 to 8.4°C and -0.4 to 17.9°C, respectively.

224 3.3 The carbon isotopes of individual *n*-alkanes

226 Our *n*-alkane-specified carbon isotope analysis of the 12 pilot samples shows a significant change.
227 Therefore, based on the chain length of the *n*-alkanes, we divided *n*-alkanes into two endmembers (Table
228 1). One is mid-chain *n*-alkanes, which had δ¹³C values ranging from -31.5 to -25.4‰ and -32.3 to -26.7‰,
229 with an average of -28.6‰ and -29.4‰ for C₂₃ and C₂₅, respectively. The other is long-chain *n*-alkanes
230 (C₂₇, C₂₉ and C₃₁), with δ¹³C values from -30.1 to -26.3‰ (C₂₇, averaging -28.0‰), -30.4 to -25.0‰ (C₂₉,
231 averaging -27.5‰) and -29.4 to -24.8‰ (C₃₁, averaging -26.9‰). The average δ¹³C values of long-chain
232 *n*-alkanes (C₂₇, C₂₉ and C₃₁) were higher than mid-chain *n*-alkanes (C₂₃ and C₂₅). C₂₆ and C₂₈ *n*-alkanes
233 had the lowest δ¹³C values averaging ~ -34‰. The percentage source of long-chain *n*-alkanes from C₃/C₄
234 plants using C₃₁ δ¹³C values varied from 47-80% for C₄ plants (Table 1).

236 4. Discussion

238 4.1 Source of mid-chain *n*-alkanes

240 Our pilot study indicates that the mid-chain *n*-alkanes (C₂₃-C₂₅) are abundant in the sediment profile,
241 and no predominant odd-over-even carbon preference is observed (CPI ~1; Fig. 2). Though contamination
242 of petroleum during coring and sampling may bring *n*-alkanes, our sampling procedures by the crew of the
243 R/V Xuelong in the 31th CHINARE have been devised to prevent any possible contamination by

244 petroleum, and no any signs of petroleum contamination have been observed while treating sediment
245 samples in the laboratory. All lab-ware was baked at 450°C in a furnace before using to prevent
246 contamination during analysis of the samples. Blank experiments were also analyzed, and negligible
247 contamination was found. Furthermore, the average $\delta^{13}\text{C}$ values of *n*-alkanes with different chain lengths
248 are different (Fig. 4). For example, the average $\delta^{13}\text{C}$ values of mid-chain *n*-alkanes (C₂₃-C₂₅) were similar
249 to the *n*-alkanes from marine phytoplankton (Ashley et al. 2020). Therefore, it is very unlikely that these
250 *n*-alkanes were due to petroleum contamination during the coring and sampling.

251 Several studies have shown that ocean phytoplankton can produce mid-chain *n*-alkanes and
252 *n*-alkanoic acids (e.g., Volkman et al. 1998). *n*-alkanoic acids are biosynthesized in the acetogenic
253 pathway and then they are converted to *n*-alkanes by enzymatic decarboxylation, thus they have similar
254 distributions (Diefendorf and Freimuth 2017). Mid-chain *n*-alkanoic acids (C₂₂-C₂₄) can be produced by
255 marine plants, such as marine microalgae, diatoms and seaweed (Naraoka and Ishiwatari 2000). Thus,
256 phytoplankton may be a significant source for these mid-chain *n*-alkanes with no predominant
257 odd-over-even carbon preference (CPI ~ 1). Previous study has reported that the average $\delta^{13}\text{C}$ values of
258 *n*-alkanoic acids produced by marine phytoplankton were about -28‰ (Ashley et al. 2020). The $\delta^{13}\text{C}$
259 values of C₂₃ and C₂₅ *n*-alkanes from C₃ plants vary from -40 to -31‰, and those from C₄ plants are in the
260 range of -23 to -18‰ (Chikaraishi et al. 2007). In our pilot analysis of the 12 samples, the average $\delta^{13}\text{C}$
261 values of *n*-alkanes with different chain length vary greatly. The $\delta^{13}\text{C}$ values of mid-chain *n*-alkanes
262 (C₂₃-C₂₅; ~ -29‰) are in the range of *n*-alkanes from marine organisms and soil samples (~ -28‰) in the
263 McMurdo Dry Valleys (Hayes et al. 1990; Ishiwatari et al. 1994; Matsumoto et al. 2010), but obviously are
264 lower than lake sediments (~ -15‰) from East Antarctica (Chen et al. 2019). Thus, terrestrial organic
265 matter from Antarctica by ice-rafted debris (IRD) and the contributions through dust transportation from
266 terrestrial ice-free areas via katabatic winds also should be considered (Chewings et al. 2014), but sources
267 from lake sediments at higher latitudes are negligible. The $\delta^{13}\text{C}$ values of C₂₆ and C₂₈ are lower relative to
268 other long-chain *n*-alkanes (Fig. 4), suggesting they may have other sources. Moreover, the $\delta^{13}\text{C}$ values of
269 C₂₆ and C₂₈ in our study samples are also obviously depleted relative to marine organisms and soil samples
270 from Antarctica. It is likely that C₂₆ and C₂₈ may originate from chemoautotrophic bacteria because they
271 have relatively low $\delta^{13}\text{C}$ values and have no odd-over-even predominance (Hayes et al. 1990; Collister et
272 al. 1994). Thus, from the above discussion, we believe that C₂₃ to C₂₅ should have mixing sources of
273 marine (non-diatom pelagic phytoplankton and marine microalgae) and terrestrial, with the marine source
274 predominant; C₂₆ and C₂₈ might be originated primarily from chemoautotrophic bacteria.

275 276 4.2 Sources of long-chain *n*-alkanes

278 There are three major sources for long-chain *n*-alkanes (C₂₇-C₃₅) in the South Pacific sector of the
279 Southern Ocean sediments including long range transport of dust from lower latitudes continent, ocean
280 plankton, and soils eroded from Antarctica. Previous studies have shown that short- and mid- chain
281 *n*-alkanes are predominant in Pleistocene age ocean sediments, water columns and suspended particulate
282 matter in the Ross Sea and Antarctic-margin, and long-chain are minor (Harada et al. 1995; Hayakawa et
283 al. 1996; Cincinelli et al. 2008). Moreover, the $\delta^{13}\text{C}$ values of *n*-alkanes ranged from -28.5 to -26.2‰,
284 suggesting that their major source was possibly derived from marine organisms (Harada et al. 1995). In the
285 Ross Sea, abundant long-chain *n*-alkanes with low CPI values in ocean sediments have suggested that the
286 organic matter was mainly originated from altered or recycled material mixed with modern marine input
287 (Kvenvolden et al. 1987; Venkatesan 1988; Duncan et al. 2019). Long range transport of terrestrial organic
288 matter and higher plant leaf waxes is also an important source for long-chain *n*-alkanes in the Pacific
289 sector of the Southern Ocean (Bendle et al. 2007; Martinez-Garcia et al. 2009, 2011; Lamy et al. 2014;
290 Jaeschke et al. 2017).

291 The core R23 is near the Antarctic continent, which is very likely be a potential source of long-chain
292 *n*-alkanes at our site. However, there are no vascular plants in the Antarctic, except for limited terrestrial
293 vegetation (moss and lichen) in relatively low latitudes of the Antarctic Peninsula. Dust contribution of
294 terrestrial material by katabatic winds is negligible due to the lack of exposed, mature soils in the
295 McMurdo Dry Valleys and Victoria Land (Nylen et al. 2004), as well as the long distance of the core site
296 from the coast. Long-chain *n*-alkanes with relatively low $\delta^{13}\text{C}$ values (-37 to -30.8‰) in the southernmost
297 Southern Ocean aerosol samples may represent a regional background of well-mixed higher vascular
298 plants through very long range transportation (Bendle et al. 2007). Moreover, Mastumoto et al. (2010)
299 have reported that the chain length of *n*-alkanes ranging from C₁₅-C₃₇ was found in McMurdo Dry Valley
300 soil, with the majority as C₂₃, C₂₅ and C₂₇ *n*-alkanes, but with extremely low abundance of C₂₉ and C₃₁
301 *n*-alkanes. Recently, Chen et al. (2019) reported that abundant long-chain *n*-alkanes with highly enriched
302 carbon isotopic ratios (~ -25 to -12‰) in lake sediments from East Antarctica (no vascular plants are
303 present in the surrounding land mass) are predominantly derived from heterotrophic microbes. However,
304 the average $\delta^{13}\text{C}$ values of long-chain *n*-alkanes (C₂₇, C₂₉ and C₃₁) varying from ~ -28 to -27‰ in the R23
305 sediments are obviously lower than these in the lake sediments from East Antarctica, as reported by Chen
306 et al. (2019). Therefore, the possibility of long-chain *n*-alkanes (C₂₇-C₃₅) via dust transport from ice-free
307 soils and lake sediments in East Antarctica and ocean phytoplankton to our site is highly unlikely.

308 The average chain length (ACL) of long-chain *n*-alkanes refers to the average number of carbon
309 atoms/molecule and can be used to indicate their source (Poynter and Eglinton 1990). The ACL values of

310 long-chain *n*-alkanes (C₂₇-C₃₅) ranged from 29.3-30.7 in the sediment samples, similar to Southern Ocean
311 ACL values with a range of 29.1-30.6 in the surface sediments, both indicating the significant contribution
312 of higher plants (Jaeschke et al. 2017). A significant linear relationship was observed between ACL and
313 CPI (n=12, r²=0.54; Fig. 3), which can help evaluate the distributional characteristics of long-chain
314 *n*-alkanes distribution. Generally, relatively high CPI values (CPI>3) indicate long-chain *n*-alkanes from
315 higher vascular plants, while low CPI values (CPI ~1) may imply mature organic matter inputs (Eglinton
316 and Eglinton 2008; Duncan et al. 2019). Based on the leaf litter degradation experiments, high
317 odd-over-even predominance declined and long-chain *n*-alkanes ratios (e.g., C₃₁/C₂₉) tended to the value of
318 ~ 1 (Zech et al. 2011). Long-chain *n*-alkanes in dust during long range transportation and deposition could
319 also be decomposed by bacteria, resulting in low CPI values. However, the δ¹³C values of long-chain
320 *n*-alkanes have no obvious difference under degradation (Huang et al. 1997; Li et al. 2017), thus it could
321 be useful to trace the sources of organic matter and reconstruct the paleoecological changes. Relatively
322 low CPI values of 1.1 to 2.5 in the R23 sediment core indicate substantial contributions of reworked
323 organic matter, which is most likely related to very low sedimentation rates <2 cm/ka (Jaeschke et al.
324 2017). Previous studies have shown that the average sedimentation rates were as low as 1.18 cm/ka in
325 Prydz Bay (Wu et al. 2015), and 1.00 cm/ka in ODP 1167 (Theissen et al. 2003). Low CPIs and low
326 sedimentation rates in the DSDP 274 sediment core from the northwest Ross Sea suggest that long-chain
327 *n*-alkanes have been extensively degraded by bacterial activity in the surface layers of the seabed (Duncan
328 et al. 2019). The high abundance of long-chain even *n*-alkanes (C₂₆ and C₂₈) with lower δ¹³C values in the
329 R23 sediment core also indicates microbial (chemoautotrophic) activity in this region. Altered or recycled
330 organic matter from Antarctica that has been eroded by glaciers and transported by ice rafted debris is
331 important in the study region (Chewings et al. 2014; Duncan et al. 2019). Therefore, we suggest that the
332 long-chain *n*-alkanes (C₂₉-C₃₅) primarily originated from terrestrial higher plant waxes via long range
333 transport of dust from lower latitude continental regions (e.g., Australia and New Zealand), and altered or
334 recycled organic matter from Antarctica may be another secondary source.

335 Our results are consistent with previous studies in the Southern Ocean, where long-chain *n*-alkanes
336 were reported to originate mainly from long range transport of dust from Australia and New Zealand by
337 prevailing westerlies (Martinez-Garcia et al. 2011; Lamy et al. 2014). For example, relatively enriched
338 carbon isotopic ratios of C₃₁ *n*-alkane in the surface sediments from the Australian sector of the Southern
339 Ocean suggest significant contributions of C₄ higher vascular plant waxes (Ohkouchi et al. 2000). More
340 recently, Jaeschke et al. (2017) have reported that the CPI values of long-chain *n*-alkanes ranged from
341 1.1-10 in the Pacific sector of the Southern Ocean, indicating the contribution of higher plant leaf waxes.
342 Because the location of surface sediments is far from the continent with the potential source regions in

343 New Zealand and Australia, it is reasonable to believe that the long-chain *n*-alkanes are primarily derive
344 from eolian transport.

346 4.3 Estimation of C₃/C₄ plant fraction

347
348 As discussed above, the long-chain *n*-alkanes (C₂₇, C₂₉ and C₃₁) in R23 sediments are primarily
349 derived from higher plant leaf waxes by long range transport of dust. Interestingly, the δ¹³C values of
350 long-chain *n*-alkanes were 5-10‰ higher than these in C₃ plants. This difference indicates that
351 considerable amounts of *n*-alkanes are derived from C₄ plant waxes which have significantly higher carbon
352 isotopic values. Many studies have shown that the δ¹³C values of long-chain *n*-alkanes of C₃ and C₄ plants
353 range from -40 to -31‰ and -23 to -18‰, respectively (Chikaraishi et al. 2007). Therefore, we can
354 quantify the percentage source of long-chain *n*-alkanes from C₃/C₄ higher plants using a binary isotope
355 mass balance model. We assumed the average δ¹³C values of long-chain *n*-alkanes for C₃ and C₄ plants to
356 be -36‰ and -22‰, respectively (Vogts et al. 2009). The relative contributions of long-chain *n*-alkanes
357 (C₂₇, C₂₉ and C₃₁) from C₃ and C₄ plants are significantly different in the sediment samples. For the carbon
358 isotopic values of C₃₁ *n*-alkanes, 80% originated from C₄ plants in the 398cm section; however, only 47%
359 originated from C₄ plants in the 762cm section (Table 1). Ohkouchi et al. (2000) reported that the relative
360 contributions of C₃₁ *n*-alkanes from C₃ and C₄ plants are about 60% and 40% in the surface sediments
361 from the Australian sector of the Southern Ocean, respectively (Ohkouchi et al. 2000). The different
362 contribution of C₃/C₄ plants may be related to the climate change (e.g. temperature and precipitation) in
363 the source regions (Huang et al. 2001). Based on the above discussion, it is reasonable to infer that the
364 source of the long-chain *n*-alkanes was mainly derived from long range transport of dust from New
365 Zealand and Australia. Therefore, this result paves the way for a future study that will allow us to analyze
366 the δ¹³C values of long-chain *n*-alkanes to reconstruct the past changes of C₃/C₄ plants in the source area.

368 4.4 Assessing U₃₇^k and U₃₇^{k'}-derived SST records

369
370 In our 12 sediment samples, C_{37:4}, C_{37:3} and C_{37:2} alkenones were all well-detected. The major alkenone
371 was C_{37:3}, with a relative abundance ranging from 27-87%. Interestingly, we also found abundant C_{37:4} in the
372 R23 sediments, ranging from 11-37%. This is similar to a previous study in higher latitude of the Pacific
373 sector of the Southern Ocean (Sikes et al. 1997), but significantly higher than the sedimentary abundance
374 from the relatively low latitude of the Southern Ocean (Jaeschke et al. 2017). Previous studies have shown
375 that C_{37:4} is often absent in open ocean sediments where SSTs are higher than 12°C (Prah et al. 1987). The

376 modern annual SST in our study site is about 0°C, thus high abundance of C_{37:4} alkenone may be related to
377 the extremely low temperature. Numerous studies have demonstrated that a high abundance of C_{37:4} in
378 surface sediments is related to low-temperature and low-salinity surface water masses in the Arctic (Sicre et
379 al. 2002; Bendle et al. 2005, 2005; Harada et al. 2006). Analysis of 106 surface water and sediment samples
380 from the Atlantic, Pacific and Southern Ocean, indicated that the relative abundance of C_{37:4} methyl
381 alkenone had no obvious relationship with SST and salinity, but it might respond to some other
382 environmental factors including growth rate, light, or nutrients (Sikes and Sicre 2002). However, most
383 samples were from the Atlantic and Pacific Oceans and there were few studies on the distributional
384 characteristics of alkenones in the high latitudes of the Southern Ocean. Moreover, the relationship of
385 temperature and salinity is strongly linear in the Atlantic and Southern Oceans, suggesting that any
386 relationship to salinity is an artifact of the covariance with temperature (Sikes and Sicre 2002).

387 To determine whether SST affects the relative abundance of C_{37:4} methyl alkenone, we calculated the
388 sea surface temperature based on the U₃₇^k and U₃₇^{k'} index using the formula reported by Prahl et al. (1988)
389 and Conte et al. (2006), respectively (Table 2). Our results show that SST data between U₃₇^k- and U₃₇^{k'}-SST
390 were, as we expected, obviously different (Fig. 5). When the relative abundance of tetra-unsaturated
391 alkenone was higher, we found U₃₇^{k'}-SST was obviously warmer than U₃₇^k-SST in 166, 243, 323, 550, 626,
392 762 and 818 cm sediment sections, and the difference between U₃₇^{k'} and U₃₇^k-SST is in the range of
393 4.8-10.9°C. Based on the average summer SST from the World Ocean Atlas (WOA09) data set (Locarnini et
394 al. 2010), the modern sea surface temperature in our study site was about 0-1°C. The U₃₇^{k'} and U₃₇^k-SST in
395 the top two samples (16 and 88 cm) are similar to modern averaged summer SST. For the historical period,
396 Ho et al. (2012) reported the difference of SSTs inferred from the U₃₇^k index between glacial and
397 interglacial periods in the Pacific sector of the Southern Ocean (54°22'S, 80°05'W) was about 7-8°C.
398 According to modern observation and the top samples, we suggest that the highest SST in our study site
399 should be lower than 7-8°C in the warmer periods, which was much lower than U₃₇^{k'}-SST. Therefore, the
400 U₃₇^{k'} index in the higher latitudes of the Southern Ocean may cause a largely warmer SST.

401 Ho et al. (2012) also found the U₃₇^{k'}-SST records were significantly warmer in glacial periods, and that
402 the U₃₇^k index is a more suitable SST proxy in the sub-Antarctic and higher latitude Pacific (Ho et al. 2012;
403 Haddam et al. 2018). Other studies have shown a significant relationship between the relative abundance of
404 C_{37:4} and temperature (Prahl et al. 1988). Moreover, several other studies indicate %C_{37:4} is closely related to
405 cold water mass expansion (Bard et al. 2000; Martínez-García et al. 2010). Although the factors influencing
406 C_{37:4} alkenone abundance in a specific location are complex, a statistically significant relationship between
407 C_{37:4} and temperature has been found if geography and low temperature are considered (Rosell-Melé et al.
408 1994, 1995). The latitude was relative high at our study site, and the modern annual summer sea surface

409 temperature was lower than 1°C. The marine algae may synthesize more C_{37:4} alkenones to adapt to the
410 extremely cold conditions. Importantly, there are few U₃₇^k-SST records in the Southern Ocean at latitudes
411 higher than 60°S. Therefore, our study indicates that the usage of U₃₇^k index is feasible for the
412 reconstruction of past SST in the Southern Ocean. Moreover, we point out here that more studies on surface
413 water and sediment samples in high latitudes are required to confirm the relationship between C_{37:4}
414 alkenones and sea surface temperature. In summary, based on our study results, long-chain *n*-alkanes are
415 primarily derived from terrestrial higher plant waxes via long range transport of dust from lower latitude
416 continental regions (e.g., Australia and New Zealand), and the U₃₇^k index can be used as a reliable index for
417 calculating sea surface temperatures in this region.

419 5. Conclusions

420
421 We have presented pilot results of the relative distribution and individual δ¹³C values of long-chain
422 *n*-alkanes and the organic geochemical characterization of alkenones in 12 samples selected from a
423 sediment core collected from the Pacific sector of the Southern Ocean. Our results suggest that the
424 abundant long-chain *n*-alkanes (C₂₇-C₃₅) with a significant odd-over-even carbon preference might have
425 originated from terrestrial higher plant waxes, possibly via long range transport of dusts from Australia and
426 New Zealand. The mid-chain *n*-alkanes (C₂₃-C₂₅) preserved in the sediments have small odd-over-even
427 carbon preference, possibly indicating mixing of marine (non-diatom pelagic phytoplankton and marine
428 microalgae) and terrestrial sources. The C₂₆ and C₂₈ *n*-alkanes with relatively lower δ¹³C values indicate an
429 origin from marine chemoautotrophic bacteria. The δ¹³C values of long-chain *n*-alkanes (C₂₇-C₃₁) range
430 between -30.8 to -24.8‰ in the sediments, approximately 5-10‰ higher than in terrestrial C₃ higher plants.
431 The carbon isotopic values of long-chain *n*-alkanes to be analyzed from the core will provide insights into
432 the history of C₃/C₄ plants in response to Pleistocene climate change. Furthermore, we found that the
433 abundances of tetra-unsaturated alkenones in the sediments are approximately 11-37%, relatively higher
434 than all those previously reported from lower latitudes adjacent to the Pacific sector of the Southern Ocean.
435 We conclude that tetra-unsaturated alkenones are sensitive markers of low SSTs, and therefore suggest the
436 feasibility of using U₃₇^k in further SST reconstructions in the Pacific sector of the Southern Ocean.

Acknowledgements

This work was jointly supported by a National Natural Science Foundation of China (grant nos. 41776188, 41576183, 41476172 and 41772366) and MOST funding (MOST 106-2116-M-019-007). We are grateful to the crew of the R/V Xuelong for their assistance with sample collection in the 31th CHINARE, and thanks to Chinese Projects for Investigations and Assessments of the Arctic and Antarctic (CHINARE2012-2020 for 01-04, 02-01 and 03-04). We also acknowledge S. Emslie for editing, and Tiegang Li for providing samples.

Author's contributions

Min-Te Chen, Xiaodong Liu and Xin Chen proposed the topic, conceived and designed the study, and they wrote the draft of this paper. Xin Chen and Da-Cheng Lin conducted the experiments. All the co-authors contributed to the discussion, and edited and commented on the paper. Linmiao Wang and Zhifang Xiong provided the chronology framework of R23 core. All authors read and approved the final manuscript.

Funding

This study was supported by grant numbers 41776188, 41576183, 41476172 and 41772366 from National Natural Science Foundation of China and the Joint Projects of MOST (Ministry of Science and Technology) to MTC. This work is also partly supported by the Chinese Projects for Investigations and Assessments of the Arctic and Antarctic (CHINARE2012-2020 for 01-04, 02-01 and 03-04) to LQC.

Availability of data and materials

The datasets in the current study are available from the corresponding author on reasonable request.

Competing interests

The authors declare that they have no competing interests.

464 **References:**

- 465 Ashley K, Bendle J, Crosta X, Etourneau J, Campagne P, Gilchrist H, Ibraheem U, Greene S, Schmidt S,
466 Eley Y, Massé G (2020) Fatty acid carbon isotopes: a new indicator of marine Antarctic
467 paleoproductivity? *Biogeosciences Discuss.* <https://doi.org/10.5194/bg-2020-124>
- 468 Bard E, Rostek F, Turon JL, Gendreau S (2000) Hydrological impact of Heinrich events in the subtropical
469 northeast Atlantic. *Science* 289:1321-1324
- 470 Bendle J, Kawamura K, Yamazaki K, Niwai T (2007) Latitudinal distribution of terrestrial lipid
471 biomarkers and n-alkane compound-specific stable carbon isotope ratios in the atmosphere over the
472 western Pacific and Southern Ocean. *Geochim Cosmochim Acta* 71:5934-5955,
- 473 Bendle J, Rosell - Melé A, Ziveri P (2005) Variability of unusual distributions of alkenones in the surface
474 waters of the Nordic seas. *Paleoceanography* 20:PA2001. <https://doi.org/10.1029/2004PA001025>
- 475 Brassell SC, Eglinton G, Marlowe IT, Pfaumann U, Sarnthein M (1986) Molecular stratigraphy: a new tool
476 for climatic assessment. *Nature* 320:129-133
- 477 Bray EE, Evans ED (1961) Distribution of n-paraffins as a clue to recognition of source beds. *Geochim*
478 *Cosmochim Acta* 22:2-15
- 479 Bubba MD, Cincinelli A, Checchini L, Lepri L, Desideri P (2004) Horizontal and vertical distributions of
480 Biogenic and Anthropogenic Organic compounds in the Ross Sea (Antarctica). *Int J Environ Anal*
481 *Chem* 8:441-456
- 482 Chen X, Liu X, Wei Y, Huang, Y (2019) Production of long chain n-alkyl lipids by heterotrophic microbes:
483 new evidence from Antarctic lakes. *Org Geochem* 138:103909.
484 <https://doi.org/10.1016/j.orggeochem.2019.103909>
- 485 Chewings JM, Atkins CB, Dunbar GB, Golledge NR (2014) Aeolian sediment transport and deposition in
486 a modern high - latitude glacial marine environment. *Sedimentology* 61:1535-1557
- 487 Chikaraishi Y, Naraoka H (2007) $\delta^{13}\text{C}$ and δD relationships among three n-alkyl compound classes
488 (n-alkanoic acid, n-alkane and n-alkanol) of terrestrial higher plants. *Org Geochem* 38:198-215
- 489 Cincinelli A, Martellini T, Bittoni L, Russo A, Gambaro A, Lepri L (2008) Natural and anthropogenic
490 hydrocarbons in the water column of the Ross Sea (Antarctica). *Journal of Marine*
491 *Systems* 73:208-220
- 492 Collister JW, Lichtfouse E, Hieshima G, Hayes JM (1994) Partial resolution of sources of n-alkanes in the
493 saline portion of the Parachute Creek Member, Green River Formation (Piceance Creek Basin,
494 Colorado). *Org Geochem* 21:645-659
- 495 Conte MH, Sicre MA, Rühlemann C, Weber JC, Shultz-Bull D, Blanz T (2006) Global temperature
496 calibration of the alkenone unsaturation index ($U_{37}^{K'}$) in surface waters and comparison with surface

497 sediments. *Geochem Geophys Geosyst* 7:Q02005. <https://doi.org/10.1029/2005GC001054>

498 Diefendorf AF, Freimuth EJ (2017) Extracting the most from terrestrial plant -derived n-alkyl lipids and
499 their carbon isotopes from the sedimentary record: A review. *Org Geochem* 103:1-21

500 Duan Y, He J (2011) Distribution and isotopic composition of n-alkanes from grass, reed and tree leaves
501 along a latitudinal gradient in China. *Geochem J* 45:199-207

502 Duncan B, McKay R, Bendle J, Naish T, Inglis GN, Moossen H, Levy R, Ventura GT, Lewis A,
503 Chamberlain B, Walker C (2019) Lipid biomarker distributions in Oligocene and Miocene sediments
504 from the Ross Sea region, Antarctica: implications for use of biomarker proxies in
505 glacially-influenced settings. *Palaeogeogr Palaeoclimatol Palaeoecol* 516:71-89

506 Eglinton TI, Eglinton G (2008) Molecular proxies for paleoclimatology. *Earth Planet Sci Lett* 275:1-16

507 Etourneau J, Collins LG, Willmott V, Kim JH, Barbara L, Leventer A, Schouten S, Sinninghe Damste JS,
508 Bianchini A, Klien V, Crosta X, Massé G (2013) Holocene climate variations in the western Antarctic
509 Peninsula: evidence for sea ice extent predominantly controlled by changes in insolation and ENSO
510 variability. *Climate of the Past* 9:1431-1446

511 Fischer H, Schmitt J, Lüthi D, Stocker TF, Tschumi T, Parekh P, Joos F, Köhler P, Völker C, Gersonde R,
512 Barbante C, Le Floch M, Raynaud D, Wolff EW (2010) The role of Southern Ocean processes in
513 orbital and millennial CO₂ variations—A synthesis. *Quat Sci Rev* 29:193-205

514 Haddam NA, Siani G, Michel E, Kaiser J, Lamy F, Duchamp-Alphonse S, Hefter J, Braconnot P, Dewilde F,
515 Isgüder G, Tisnerat-Laborde N, Thil F, Durand N, Kissel C (2018) Changes in latitudinal sea surface
516 temperature gradients along the Southern Chilean margin since the last glacial. *Quat Sci*
517 *Rev* 194:62-76

518 Harada N, Handa N, Fukuchi M, Ishiwatari R (1995) Source of hydrocarbons in marine sediments in
519 Lützow-Holm Bay, Antarctica. *Org Geochem* 23:229-237

520 Harada N, Sato M, Shiraishi A, Honda MC (2006) Characteristics of alkenone distributions in suspended
521 and sinking particles in the northwestern North Pacific. *Geochim Cosmochim Acta* 70:2045-2062

522 Hayakawa K, Handa N, Ikuta N, Fukuchi M (1996) Downward fluxes of fatty acids and hydrocarbons
523 during a phytoplankton bloom in the austral summer in Breid Bay, Antarctica. *Org*
524 *Geochem* 24:511-521

525 Hayes JM, Freeman KH, Popp BN, Hoham CH (1990) Compound-specific isotopic analyses: a novel tool
526 for reconstruction of ancient biogeochemical processes. *Org Geochem* 16:1115-1128

527 Ho SL, Mollenhauer G, Lamy F, Martinez-Garcia A, Mohtadi M, Gersonde R, Hebbeln D, Nunez-Ricardo
528 S, Rosell-Mele A, Tiedemann R (2012) Sea surface temperature variability in the Pacific sector of the
529 Southern Ocean over the past 700 kyr. *Paleoceanography* 27:PA4202.

530 <https://doi.org/10.1029/2012PA002317>

531 Holtvoeth J, Whiteside JH, Engels S, Freitas FS, Grice K, Greenwood P, Johnson S, Kendall I, Lengger
532 SK, Lücke A, Mayr C, Naafs BDA, Rohrsen M, Sepúlveda J (2019) The paleolimnologist's guide to
533 compound-specific stable isotope analysis – An introduction to principles and applications of CSIA
534 for Quaternary lake sediments. *Quat Sci Rev* 207:101–133

535 Huang Y, Eglinton G, Ineson P, Latter PM, Bol R, Harkness DD (1997) Absence of carbon isotope
536 fractionation of individual n-alkanes in a 23-year field decomposition experiment with *Calluna*
537 *vulgaris*. *Org Geochem* 26:497-501

538 Huang Y, Street-Perrott FA, Metcalfe SE, Brenner M, Moreland M, Freeman K (2001) Climate change as
539 the dominant control on glacial-interglacial variations in C₃ and C₄ plant
540 abundance. *Science* 293:1647-1651

541 Ishiwatari R, Uzaki M, Yamada K (1994) Carbon isotope composition of individual n-alkanes in recent
542 sediments. *Org Geochem* 21:801-808

543 Jaeschke A, Wengler M, Hefter J, Ronge TA, Geibert W Mollenhauer G, Lamy F (2017) A biomarker
544 perspective on dust, productivity, and sea surface temperature in the Pacific sector of the Southern
545 Ocean. *Geochim Cosmochim Acta* 204:120-139

546 Kim JH, Crosta X, Willmott V, Renssen H, Bonnin J, Helmke P, Schouten S, Sinninghe Damste JS (2012)
547 Holocene subsurface temperature variability in the eastern Antarctic continental margin. *Geophys Res*
548 *Lett* 39:L06705. <https://doi.org/10.1029/2012GL051157>

549 Kohfeld KE, Graham RM, De Boer AM, Sime LC, Wolff EW, Le Quéré C, Bopp L (2013) Southern
550 Hemisphere westerly wind changes during the Last Glacial Maximum: paleo-data synthesis. *Quat Sci*
551 *Rev* 68:76-95

552 Kvenvolden KA, Rapp JB, Golan-Bac M, Hostettler FD (1987) Multiple sources of alkanes in Quaternary
553 oceanic sediment of Antarctica. *Org Geochem* 11:291-302

554 Lamy F, Gersonde R, Winckler G, Esper O, Jaeschke A, Kuhn G, Ullermann J, Martínez-García A,
555 Lambert F, Kilian R (2014) Increased dust deposition in the Pacific Southern Ocean during glacial
556 periods. *Science* 343:403-407

557 Lamy F, Kilian R, Arz HW, Francois JP, Kaiser J, Prange M, Steinke T (2010) Holocene changes in the
558 position and intensity of the southern westerly wind belt. *Nat Geosci* 3:695-699

559 Li R, Fan J, Xue J, Meyers PA (2017) Effects of early diagenesis on molecular distributions and carbon
560 isotopic compositions of leaf wax long chain biomarker n-alkanes: Comparison of two one-year-long
561 burial experiments. *Org Geochem* 104:8-18

562 Lisiecki LE, Raymo ME (2005) A Pliocene-Pleistocene stack of 57 globally distributed benthic $\delta^{18}\text{O}$
563 records, *Paleoceanography* 20:PA1003. doi:10.1029/2004PA001071

564 Locarnini RAM, Antonov JI, Boyer TP, Garcia HE, Baranova OK, Zweng MM, Johnson DR (2010) World
565 Ocean Atlas 2009: Volume 1: Temperature. In NOAA Atlas NESDIS 68 (ed. S. Levitus). U.S.
566 Government Printing Office, Washington D.C. p. 184

567 Marshall J, Speer K (2012) Closure of the meridional overturning circulation through Southern Ocean
568 upwelling. *Nat Geosci* 5:171-180

569 Martínez - Garcia A, Rosell - Melé A, Geibert W, Gersonde R, Masqué P, Gaspari V, Barbante C (2009)
570 Links between iron supply, marine productivity, sea surface temperature, and CO_2 over the last 1.1
571 Ma. *Paleoceanography* 24:PA1207. <https://doi.org/10.1029/2008PA001657>

572 Martinez-Garcia A, Rosell-Melé A, Jaccard SL, Geibert W, Sigman DM, Haug GH (2011) Southern Ocean
573 dust-climate coupling over the past four million years. *Nature* 476:312-315

574 Matsumoto GI, Honda E, Sonoda K, Yamamoto S, Takemura T (2010) Geochemical features and sources
575 of hydrocarbons and fatty acids in soils from the McMurdo Dry Valleys in the Antarctic. *Polar*
576 *Sci* 4:187-196

577 Meyers PA, Ishiwatari R (1993) Lacustrine organic geochemistry—an overview of indicators of organic
578 matter sources and diagenesis in lake sediments. *Org Geochem* 20:867-900

579 Naraoka H, Ishiwatari R (2000) Molecular and isotopic abundances of long-chain n-fatty acids in open
580 marine sediments of the western North Pacific. *Chem. Geol* 165:23-36

581 Nylen TH, Fountain AG, Doran PT (2004) Climatology of katabatic winds in the McMurdo dry valleys,
582 southern Victoria Land, Antarctica. *J Geophys Res: Atmos* 109:D03114.
583 <https://doi.org/10.1029/2003JD003937>

584 Ohkouchi N., Kawamura K., Takemoto N., Ikehara M. & Nakatsuka T. 2000. Implications of carbon
585 isotope ratios of C_{27} - C_{33} alkanes and C_{37} alkenes for the sources of organic matter in the southern
586 ocean surface sediments. *Geophys Res Lett* 27:233-236

587 Pahnke K, Zahn R (2005) Southern Hemisphere water mass conversion linked with North Atlantic climate
588 variability. *Science* 307:1741-1746

589 Poynter J, Eglinton G (1990) Molecular composition of three sediments from Hole 717C: the Bengal Fan.
590 In: Cochran, J.R., Stow, D.A.V., et al. (Eds.), *Proceedings of Ocean Drilling Program, Scientific*
591 *Results*, vol. 166. College Station, TX (Ocean Drilling Program), pp. 155–161

592 Prah FG, Muehlhausen LA, Zahnle DL (1988) Further evaluation of long-chain alkenones as indicators of
593 paleoceanographic conditions. *Geochim Cosmochim Acta* 52:2303-2310

594 Prah FG, Wakeham SG (1987) Calibration of unsaturation patterns in long-chain ketone compositions for

595 palaeotemperature assessment. *Nature* 330:367-369

596 Rosell-Melé A, Carter J, Eglinton G (1994) Distributions of long-chain alkenones and alkyl alkenoates in
597 marine surface sediments from the North East Atlantic. *Org Geochem* 22:501-509

598 Rosell-Melé A, Eglinton G, Pflaumann U, Sarnthein M (1995) Atlantic core-top calibration of the U_{37}^K
599 index as a sea-surface palaeotemperature indicator. *Geochim Cosmochim Acta* 59:3099-3107

600 Shevenell AE, Ingalls AE, Domack EW, Kelly C (2011) Holocene Southern Ocean surface temperature
601 variability west of the Antarctic Peninsula. *Nature* 470:250-254

602 Sicre MA, Bard E, Ezat U, Rostek F (2002) Alkenone distributions in the North Atlantic and Nordic sea
603 surface waters. *Geochem Geophys Geosyst* 3. <https://doi.org/10.1029/2001GC000159>

604 Sikes EL, Sicre MA (2002) Relationship of the tetra - unsaturated C37 alkenone to salinity and
605 temperature: Implications for paleoproxy applications. *Geochem Geophys Geosyst* 3.
606 <https://doi.org/10.1029/2001GC000159>

607 Sikes EL, Volkman JK (1993) Calibration of alkenone unsaturation ratios (U_{37}^k) for paleotemperature
608 estimation in cold polar waters. *Geochim Cosmochim Acta* 57:1883-1889

609 Sikes EL, Volkman JK, Robertson LG, Pichon JJ (1997) Alkenones and alkenes in surface waters and
610 sediments of the Southern Ocean: Implications for paleotemperature estimation in polar
611 regions. *Geochim Cosmochim Acta* 61:1495-1505

612 Theissen KM, Dunbar RB, Cooper AK, Mucciarone DA, Hoffmann D (2003) The Pleistocene evolution of
613 the East Antarctic Ice Sheet in the Prydz Bay region: stable isotopic evidence from ODP Site
614 1167. *Global and Planetary Change* 39:227-256

615 Thomas EK, Huang Y, Morrill C, Zhao J, Wegener P, Clemens SC, Colman SM, Gao L (2014) Abundant
616 C4 plants on the Tibetan Plateau during the late glacial and early Holocene. *Quat Sci Rev* 87:24–33

617 Toggweiler JR, Russell J (2008) Ocean circulation in a warming climate. *Nature* 451:286-288

618 Toyos MH, Lamy F, Lange CB, Lembke-Jene L, Saavedra-Pellitero M, Esper O, Arz HW (2020) Antarctic
619 circumpolar current dynamics at the Pacific entrance to the Drake Passage over the past 1.3
620 million years. *Paleoceanography and Paleoclimatology* 35:e2019PA003773.
621 <https://doi.org/10.1029/2019PA003773>

622 Venkatesan MI (1988) Organic geochemistry of marine sediments in Antarctic region: Marine lipids in
623 McMurdo Sound. *Org Geochem* 12:13-27

624 Vogts A, Moossen H, Rommerskirchen F, Rullkötter J (2009) Distribution patterns and stable carbon
625 isotopic composition of alkanes and alkan-1-ols from plant waxes of African rain forest and savanna
626 C₃ species. *Org Geochem* 40:1037-1054

627 Volkman JK, Barrett SM, Blackburn SI, Mansour MP, Sikes EL, Gelin F (1998) Microalgal biomarkers: a

628 review of recent research developments. *Org Geochem* 29:1163-1179

629 Wu Li, Wang Rujian, Xiao Wenshen, Ge Shulan, Chen Zhihua (2015) High resolution age model of Late
630 Quaternary Mouth Fan at Prydz Trough, Eastern Antarctic. *Marine Geology and Quaternary Geology*
631 (in Chinese with English abstract) 35:197-208

632 Yamamoto M, Shiraiwa Y, Inouye I (2000) Physiological responses of lipids in *Emiliana huxleyi* and
633 *Gephyrocapsa oceanica* (Haptophyceae) to growth status and their implications for alkenone
634 paleothermometry. *Org Geochem* 31:799-811

635 Zech M, Pedentchouk N, Buggle B, Leiber K, Kalbitz K, Marković SB, Glaser B (2011) Effect of leaf
636 litter degradation and seasonality on D/H isotope ratios of n-alkane biomarkers. *Geochim Cosmochim*
637 *Acta* 75:4917-4928

638

639 Table 1 Concentrations, $\delta^{13}\text{C}$ values and typical indices based on *n*-alkanes in the subsamples with
640 different sediment depth. The relative contribution of long chain *n*-alkanes from C_3 and C_4 plants are
641 calculated by carbon isotopes of the C_{31} *n*-alkane.

Depth (cm)	$\delta^{13}\text{C}_{23}$ (‰)	$\delta^{13}\text{C}_{24}$ (‰)	$\delta^{13}\text{C}_{25}$ (‰)	$\delta^{13}\text{C}_{26}$ (‰)	$\delta^{13}\text{C}_{27}$ (‰)	$\delta^{13}\text{C}_{28}$ (‰)	$\delta^{13}\text{C}_{29}$ (‰)	$\delta^{13}\text{C}_{31}$ (‰)	<i>n</i> -alkanes ^a (ng/g)	C_4 (%)	C_3 (%)	ACL ^b	CPI ^c
16	-29.6	-28.8	-29.9	-33.2	-28.5	-32.2	-27.4	-28.3	445	55	45	30.1	1.6
88	-29.5	-31.8	-27.3	-30.0	-26.3	-33.1	-25.1	-25.5	328	75	25	30.3	2.0
166	-25.4	-26.4	-26.7	-32.5	-28.3	-38.0	-27.1	-27.8	295	59	41	30.1	2.1
243	-27.1	-26.8	-26.8	-30.4	-26.7	-33.3	-29.8	-28.3	362	55	45	30.3	2.5
323	-29.8	-31.2	-30.6	-35.0	-28.3	-32.1	-29.4	-27.9	324	58	42	29.3	1.3
398	-31.5	-35.9	-30.0	-36.7	-28.6	-34.6	-25.0	-24.8	787	80	20	29.6	1.3
482	-26.8	-28.4	-29.3	-30.3	-26.8	-30.1	-27.4	-26.6	411	67	33	30.7	1.9
550	-27.1	-30.7	-29.3	-35.1	-27.8	-31.2	-27.8	-25.4	420	76	24	30.1	1.6
626	-30.4	-32.2	-31.7	-34.6	-29.6	-30.9	-26.4	-25.8	344	73	27	29.6	1.6
698	-28.6	-30.6	-29.0	-32.7	-27.8	-31.8	-27.0	-25.8	490	73	27	29.3	1.1
762	-28.8	-29.3	-30.0	-35.3	-26.7	-32.1	-30.4	-29.4	455	47	53	29.8	1.6
818	-28.8	-28.7	-32.3	-37.4	-30.1	-35.8	-27.7	-27.2	503	63	37	30.1	1.7

642

643 a: Total concentrations of C_{23} - C_{35} *n*-alkanes

644 b: $\text{ACL}_{27-35} = \sum(i \times X_i) / \sum X_i$, where X is abundance and i ranges from C_{27} - C_{35} odd *n*-alkanes

645 c: $\text{CPI}_{27-33} = 0.5 \times \sum(\text{C}_{27}\text{-C}_{33}) / (\text{C}_{26}\text{-C}_{32}) + 0.5 \times \sum(\text{C}_{27}\text{-C}_{33}) / (\text{C}_{28}\text{-C}_{34})$

646

647 Table 2 The relative abundance and concentrations of C_{37:4}, C_{37:3} and C_{37:2} alkenones and based on U₃₇^k-
 648 and U₃₇^{k'}-SST in the subsamples with different sediment depth.

Depth	C _{37:4}	C _{37:3}	C _{37:2}	Alkenones	U ₃₇ ^k -SST ^a	U ₃₇ ^{k'} -SST ^b
(cm)	(%)	(%)	(%)	(ng/g)	(°C)	(°C)
16	12	85	4	90.7	0.6	-0.1
88	11	87	3	104.2	0.7	-0.4
166	30	40	30	13.2	2.8	11.5
243	21	51	28	15.3	4.4	9.2
323	35	48	17	14.7	-1.7	6.6
398	16	64	19	50.1	3.5	5.6
482	15	80	6	65.1	0.5	0.7
550	37	38	24	12.6	-0.6	10.3
626	30	44	26	14.0	1.8	9.9
698	23	59	18	19.1	1.2	5.7
762	25	27	48	30.2	8.4	17.9
818	30	36	34	19.0	3.6	13.2

649

650 a: $U_{37}^{k'} = C_{37:2} / (C_{37:2} + C_{37:3})$

651 b: $U_{37}^k = (C_{37:2} - C_{37:4}) / (C_{37:2} + C_{37:3} + C_{37:4})$

652

653 FIGURE CAPTIONS:

654
655 Fig. 1. Map of the Southern Ocean and the continent of Antarctica. Red pentagram denotes the site of the
656 sediment core in our study. Red triangles indicate sites of sea surface temperature or sea subsurface
657 temperature records reported in previous studies. The SST record in the PS75/034-2 sediment core was
658 used for the U_{37}^k index (Ho et al., 2012), whereas other sediment cores (ODP 1098, JPC 10 and
659 MD03-2601) were used for TEX_{86} (Shevenell et al., 2011; Kim et al., 2012; Etourneau et al., 2013). The
660 thick blue line indicates the Antarctic Circumpolar Current (ACC). The solid dots denote ice core locations
661 in the Antarctic, including Dome C and Vostok.

662
663 Fig. 2. The relative abundance of long chain *n*-alkanes (C_{23} - C_{35}) at different depths of the sedimentary
664 section.

665
666 Fig. 3. Relationship between ACL_{27-35} and CPI_{27-33} of long chain *n*-alkanes.

667
668 Fig. 4. The average $\delta^{13}C$ values of *n*-alkanes. Error bars represent 1 standard deviation of 12 samples.

669
670 Fig. 5. The relative abundance of $C_{37:4}$, $C_{37:3}$ and $C_{37:2}$ alkenones and the calculated sea surface
671 temperature based on U_{37}^k and $U_{37}^{k'}$ index at different depths of the sedimentary section. The light grey
672 and light blue bands represent modern average summer SST and highest SST during the Holocene at the
673 same latitude of the Southern Ocean, respectively. The age of R23 core is cited from Wang et al.
674 (unpublished data).

675

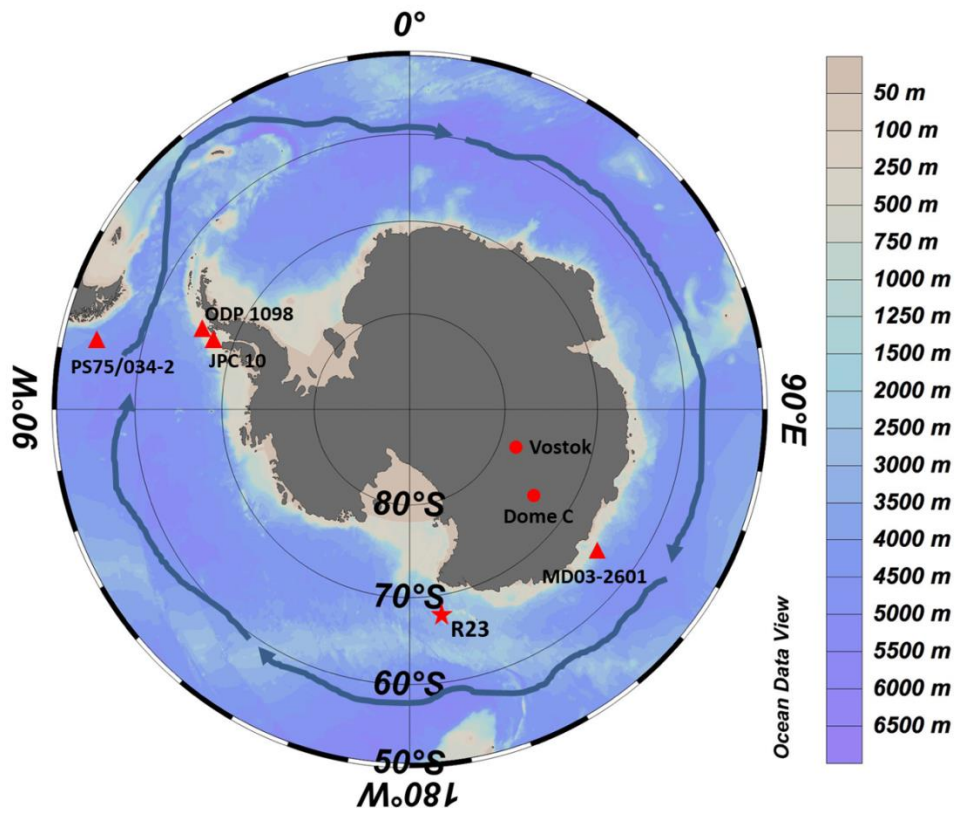


Figure 1

676
 677
 678
 679

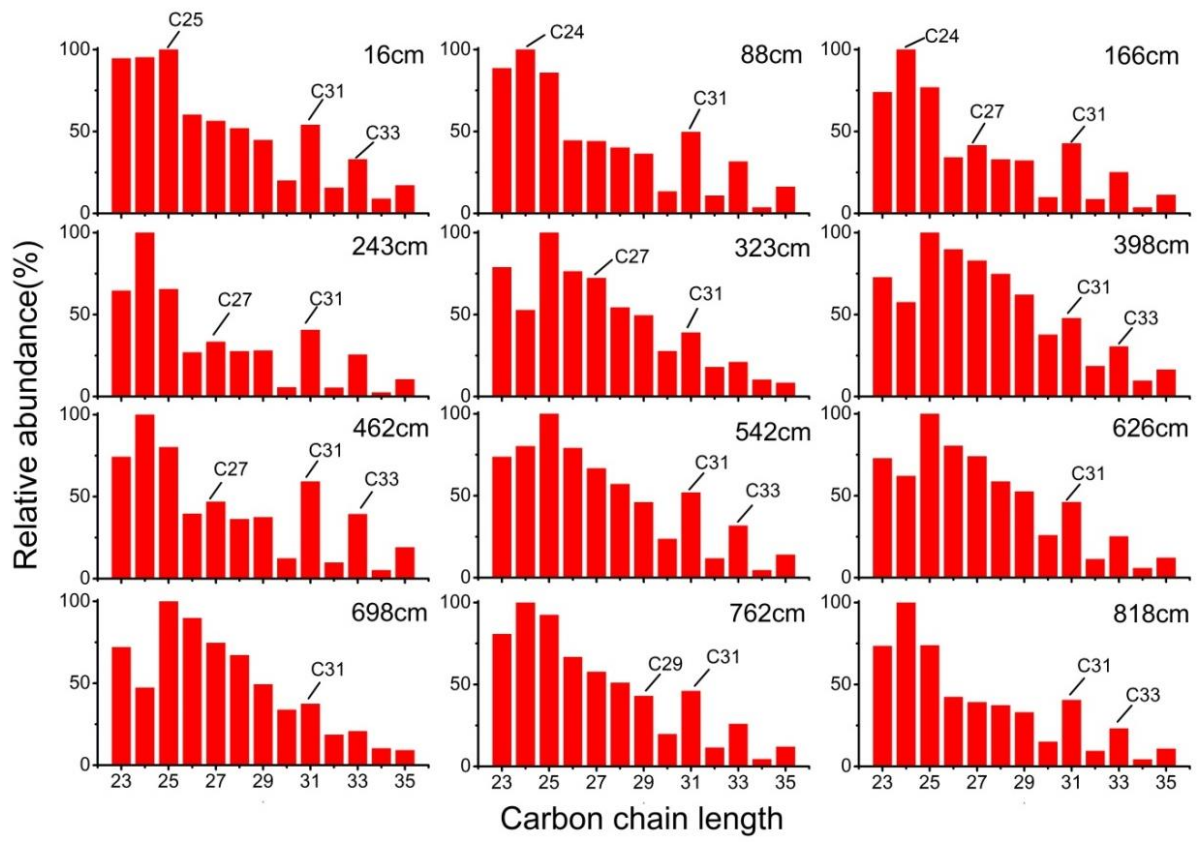
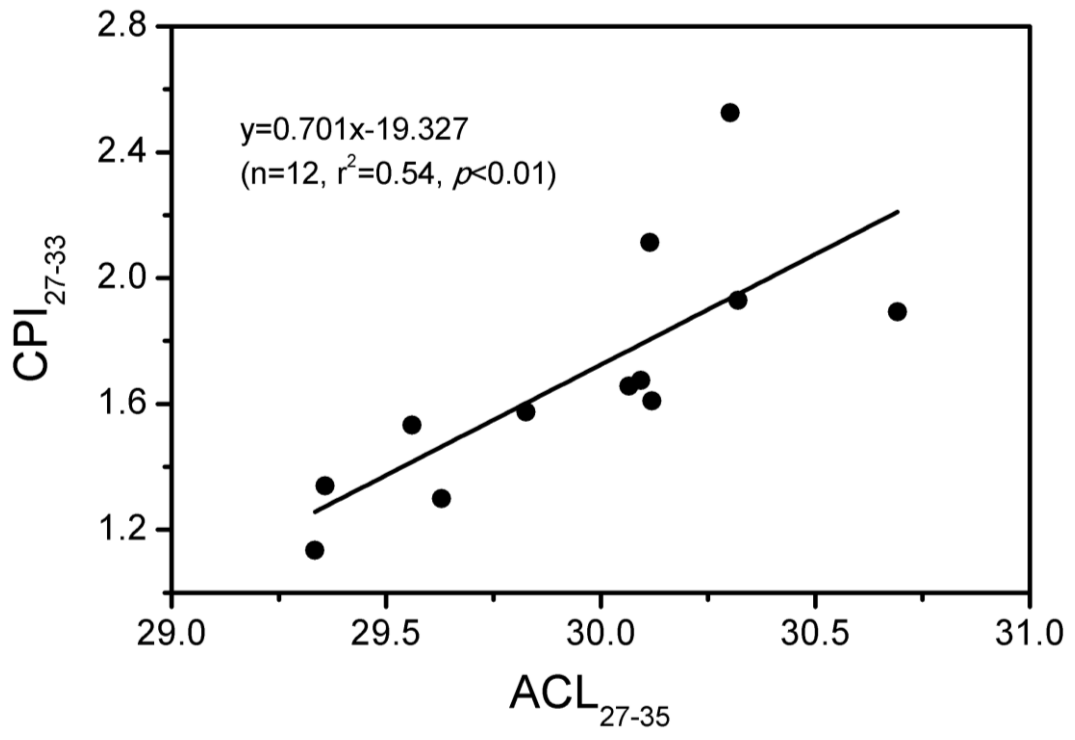


Figure 2

680
681
682
683



684
685
686
687

Figure 3

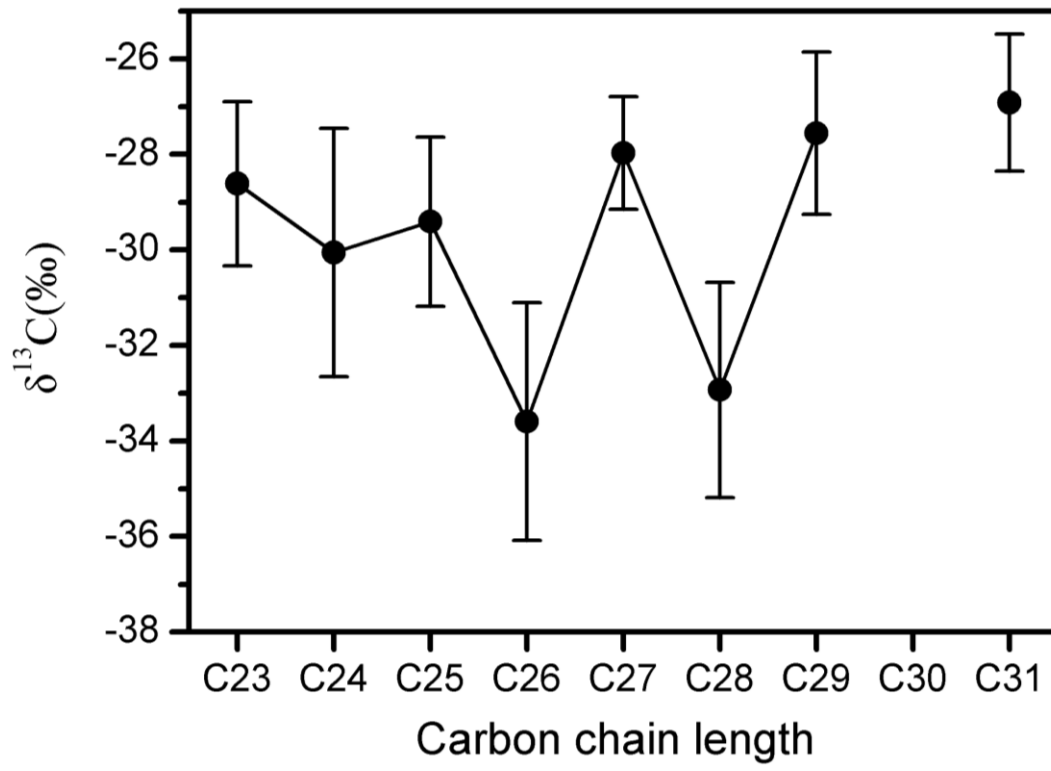


Figure 4

688
689
690
691

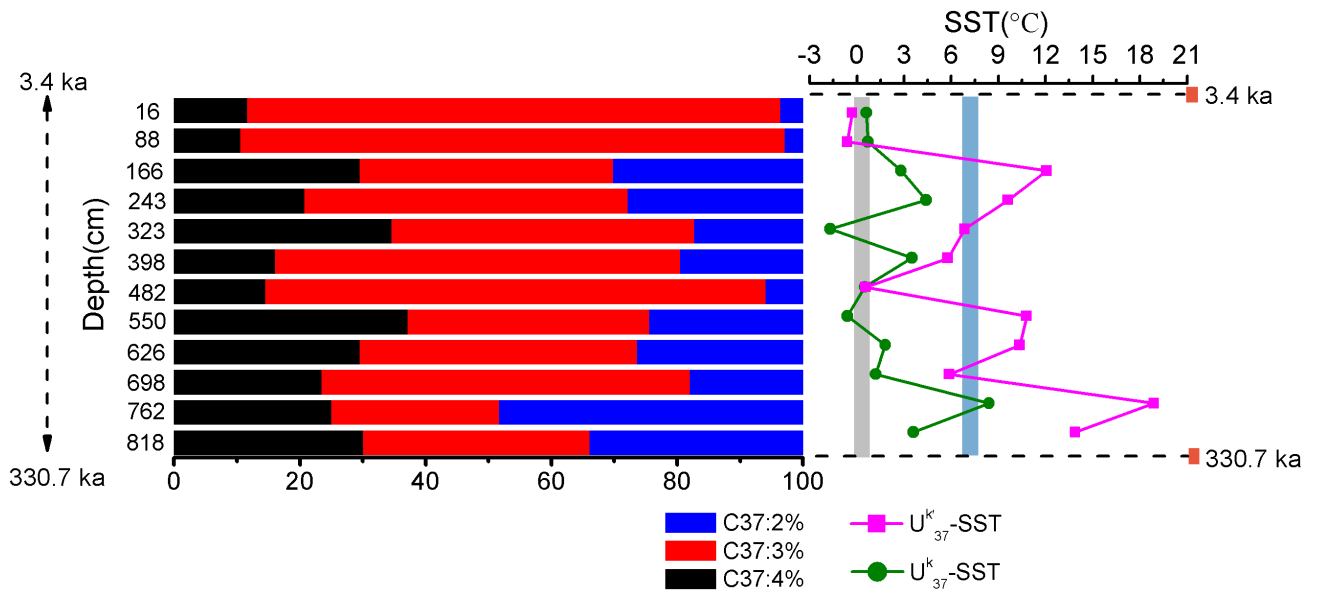


Figure 5

692
693
694
695